Springer

Journal of Mechanical Science and Technology 23 (2009) 1702~1709

Journal of Mechanical Science and Technology

www.springerlink.com/content/1738-494x
DOI 10.1007/s12206-009-0413-5

Numerical analysis of the subsonic flow around a three-dimensional cavity †

Hong-il Choi[1], Pa-ul Mun[2] and Jae-soo Kim[2,*]

[1]*Korea Electric Power Research Institute 103-14, Munji-Dong, Yusong-Ku, Taejeon, 305-380, Korea*
[2]*Department of Aerospace Engineering, Chosun University, 375 Seosuk-dong, Dong-gu, Gwangju, 501-759, Korea*

(Manuscript Received September 1, 2008; Revised January 5, 2009; Accepted February 15, 2009)

Abstract

Flight vehicles such as wheel wells and bomb bays have many cavities. The flow around a cavity is characterized as an unsteady flow because of the formation and dissipation of vortices brought about by the interaction between the free stream shear layer and the internal flow of the cavity. The resonance phenomena can damage the structures around the cavity and negatively affect the aerodynamic performance and stability of the vehicle. In this study, a numerical analysis was performed for the cavity flows using the unsteady compressible three-dimensional Reynolds-Averaged Navier-Stokes (RANS) equation with Wilcox's turbulence model. The Message Passing Interface (MPI) parallelized code was used for the calculations by PC-cluster. The cavity has aspect ratios (*L/D*) of 2.5 ~ 7.5 with width ratios (*W/D*) of 2 ~ 4. The Mach and Reynolds numbers are 0.4 ~ 0.6 and 1.6×10^6, respectively. The occurrence of oscillation is observed in the "shear layer and transient mode" with a feedback mechanism. Based on the Sound Pressure Level (SPL) analysis of the pressure variation at the cavity trailing edge, the dominant frequencies are analyzed and compared with the results of Rossiter's formula. The dominant frequencies are very similar to the result of Rossiter's formula and other experimental data in the low aspect ratio cavity (*L/D* = ~ 4.5). In the large aspect ratio cavity, however, there are other low dominant frequencies due to the leading edge shear layer with the dominant frequencies of the feedback mechanism. The characteristics of the acoustic wave propagation are analyzed using the Correlation of Pressure Distribution (CPD).

Keywords: Unsteady subsonic flow; $k-\omega$ Turbulence model; Three dimensional cavity flow; Sound pressure level; Correlation of pressure distribution

1. Introduction

Generally, flight vehicles have many cavities in their bodies such as wheel wells, bomb bays, and windows on their external surfaces. The flow around these cavities creates separation, vortex, shock and expansion waves, reattachment, and other complex flow phenomena. The flow around a cavity makes noise and vibration even though the aspect ratio (*L/D*) is small. The cavity may make tremendous noise and have structural damage, breakage, or aerodynamic instability. Thus, many studies have been conducted to understand precisely and interpret the flow around the cavity. Such studies have also been carried out to reduce the noise and vibration. Currently, many researchers are trying to adopt state-of-the-art technology in this area.

The flow around a cavity can be divided mainly into two categories: open type (*L/D*<10) flow and closed type (*L/D*>13) flow. The closed type flow creates a shear layer on the leading edge of the cavity, which impacts on and reflects from the bottom and exits out of the downstream edge of the cavity. During this process, two small separated zones are formed to prevent severe resonance. On the other hand, the open type flow creates severe vibration due

† This paper was recommended for publication in revised form by Associate Editor Do Hyung Lee
*Corresponding author. Tel.: +82 62 230 7080, Fax.: + 82 62 223 8894
E-mail address: jsckim@chosun.ac.kr

to the pressure change caused by the interactivity of the internal and external flows. The shear layer generated on the leading edge of the cavity reattaches itself on the downstream edge and unstably blocks the internal and external flow [1].

Krishnamurty [2], Rossiter [3], and Heller [4] showed that the intensity of the vibration depends on factors such as the boundary layer coming into the cavity, the shape of cavity, and flow speed, among many others. Gharib and Roshko [5] numerically demonstrated that the shear layer mode changes to the wake mode as the aspect ratio (the ratio of length and depth, *L/D*) increases in the two-dimensional cavity flow. It is shown that the shear layer mode is more dominant than the wake mode in the three-dimensional cavity flow [6]. Although the shear layer hits the downstream edge in the shear layer mode, the layer hits the bottom of the cavity and exits out of the downstream of the cavity in the wake mode, the occurrence of which leads to severe vibrations.

In this study, the unsteady compressible Reynolds-Averaged Navier-Stokes (RANS) equation was used with Wilcox's turbulence model. For numerical analysis, a fourth-order Runge-Kutta time discretization and a Flux Vector Split (FVS) method with van Leer's limit as spatial discretization were used. From the numerical results, an acoustic field was analyzed for the generation and propagation according to the aspect ratio and span-wise variation of the cavity. The results of the Strouhal number (St) were compared with the results of the Rossiter equation and the experimental results of Ahuja and Mendoza [8]. The Sound Pressure Level (SPL) was analyzed with Fast Fourier transform (FFT) for the dominant frequencies of the cavity flow. The dominant frequencies are very similar to the results of Rossiter's formula and other experiments in the low aspect ratio cavity (*L/D*= ~ 4.5). In the large aspect ratio cavity, however, there are other low dominant frequencies due to the leading edge shear layer with the dominant frequencies of the feedback mechanism. In the low *L/D* cavity, the vortex flowing from the trailing edge dominates the flow characteristics inside the cavity and the shear layer vibration. In the large *L/D* cavity, however, the vortex flowed from the trailing edge, and the interference by the vortex generated at the leading edge jointly dominates the flow characteristics inside the cavity. Frequency analysis also shows that the main dominant frequencies appear due to the feedback mechanism, while the low frequency appears due to the vibration of the middle-stage shear layer. Meanwhile, we also analyzed the Correlation of Pressure Distribution (CPD), which can indicate the pressure correlation between the reference point and other areas, in order to show the propagation process of the pressure waves [15].

2. Governing equation and numerical analysis

The non-dimensionalized three-dimensional Navier-Stokes equation is written as follows:

$$\frac{\partial \bar{Q}}{\partial t}+\frac{\partial \bar{E}}{\partial \xi}+\frac{\partial \bar{F}}{\partial \eta}+\frac{\partial \bar{G}}{\partial \zeta}=\frac{\partial \bar{E}_V}{\partial \xi}+\frac{\partial \bar{F}_V}{\partial \eta}+\frac{\partial \bar{G}_V}{\partial \zeta}+\bar{S}\,. \quad (1)$$

The cavity depth (*D*), free stream velocity, and free stream density are the non-dimensional reference values, while t,ξ,η, and ζ are the time and generalized coordinates. $\bar{Q}$ is a non-dimensional conserved flux vector transferred to the generalized coordinates, while $\bar{E},\bar{F},\bar{G},\bar{E}_v,\bar{F}_v$, and $\bar{G}_v$ are generalized coordinate flux vectors expressed by the transformation matrix and flux vectors. Refer to the reference literatures [9] for the non-viscosity flux vectors Q,E,F,G, viscosity flux vectors E_V,F_V,G_V, and other symbols. Finally, $\bar{S}$ is used to calculate the turbulence model equation.

Wilcox's $k-\omega$ model [10] is used as a turbulence model. The turbulence kinetic energy and the dissipation rate can be formulated in the generalized coordinates as a non-dimensional conservation type similar to the Navier-Stokes Eq. [15]. This model was developed to calculate the incompressible flow and expand to the compressible flow. Bardina, Huang, and Coakley [11] showed that Wilcox's model can be properly applied to the compressible flow in their turbulence model comparison study.

For the time discretization, an explicit fourth-order Runge-Kutta method was used. On the other handm for spatial discretization, a second-order Flux Vector Split (FVS) method with van Leer's flux limiter was used. The numerical calculation was carried out through MPI techniques using a PC-cluster of 20 PCs.

3. Results and discussion

A three-dimensional numerical analysis was conducted to observe the flow phenomena around a single cavity. The configuration and flow conditions are basically the same as the results in Ahuja and Men-

doza [8]'s test model. The cavity depth (D) of 5.08 cm and the Mach number of 0.4 ~ 0.6 were used. The aspect ratio (L/D) and the width to depth ratio (W/D) were found to be at 2.5 ~ 7.5, and 2.0 ~ 4.0, respectively.

Fig. 1 shows a part of the computational grid for three-dimensional calculation. The grids are concentrated around the wall. As ($y^+ = (y\sqrt{\rho_\omega \tau_\omega}/\mu_\omega$) of the first grid point is about 0.01 ~ 1.5, the calculation can be directly conducted without using a wall function. Abdol-Hamid et al. [12] showed that the results are reasonable if y^+ of the first gird point is less than 10 in the flow containing a relatively large separated zone. To verify the effect of the number of grids, several sets of grids were tested. For the two-dimensional calculation, the grids of 350×100 in the main stream and 100×70 in the cavity area are used, while the grids of $190 \times 70 \times 50$ and $70 \times 50 \times 30$ for the three-dimensional calculation were also used. For the analysis of the dynamic characteristics, the $SPL(f)$ at the center point of downstream edge was analyzed through FFT analysis using Eq. (2) to obtain the dominant frequencies. The pressure wave propagation characteristics were observed by the $\mathrm{Re}(CPD(f))$ of the dominant frequencies between the center of the downstream edge as a reference point and other areas [15].

$$SPL(f) = 20\log_{10}(FFT(p)/p_{ref})(dB) \quad (2)$$

$$\mathrm{Re}(CPD(f)) = 10\log_{10}(\mathrm{Re}((FFT_{ref}(p)/p_{ref}) \bullet (FFT(p)/p_{ref})))(dB)$$

$$p_{ref} = 2\times10^{-5}(N/m^2)$$

where f, p and p_{ref} are the frequency, pressure, and reference sound pressure, respectively.

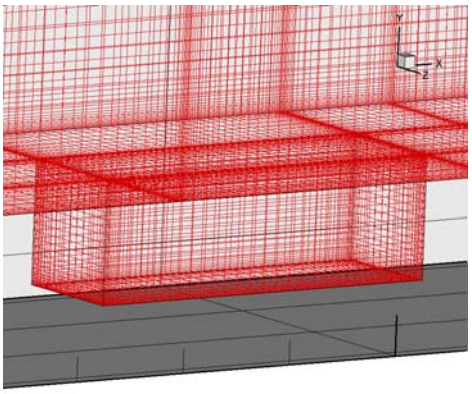

Fig. 1. Computational grid for the three-dimensional calculation.

The cases in this study basically correspond to the shear layer mode, which is one of the three modes aside from the steady mode and wake mode mentioned in Gharib [5]. The shear layer created at the leading edge will propagate along the flow and become gradually amplified. When this shear layer hits the wall of the downstream edge, it creates a strong pressure wave, which will become a noise source. A part of the acoustic wave propagates upward and interacts with the shear layer coming from the leading edge. Fig. 2 shows that the vortex generated in the shear layer of the leading edge hits the downstream edge and is divided into several vortices, some of which flow along the wall outside the cavity in the direction of the downstream while some flow into the cavity. Due to the vortices flowing into the cavity, one big vortex is created at the rear of the cavity. This big vortex will interact with the shear layer, creating a severe vibration of the cavity flow. Fig. 3 shows how the acoustic waves propagate upstream.

Meanwhile, Fig. 4 shows that a shear layer is created at the leading edge and propagated to the downstream edge with the streamlines. These are the density contours and streamlines in one cycle inside the cavity at the center section of the three-dimensional cavity.

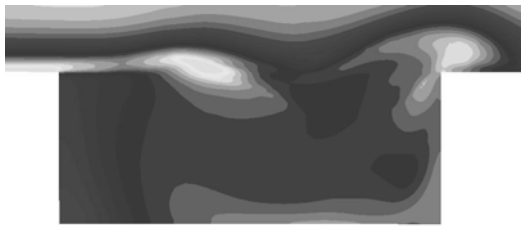

Fig. 2. Density contours of the shear layer mode.

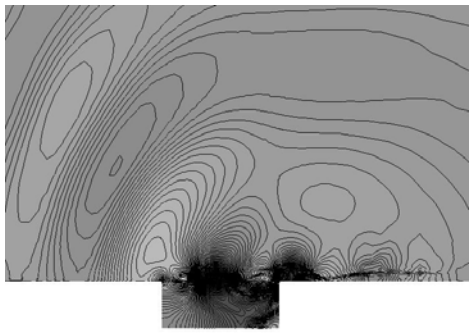

Fig. 3. Acoustic field of the entire domain *(M=0.53, L/D=2.5, Re=1.6×10⁶).*

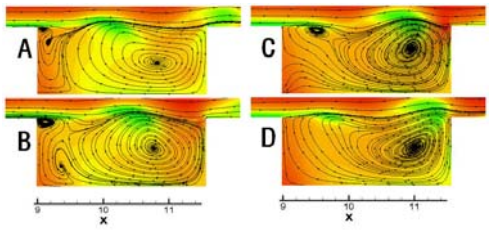

Fig. 4. Streamlines and density contours at the center section of the three-dimensional cavity *(L/D=2.5)*.

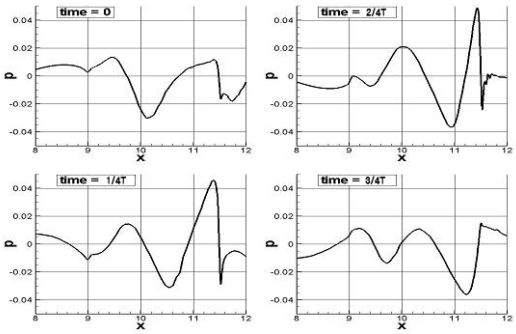

Fig. 5. Pressure signals along the x-direction at y=1.02D.

The shear layer created at the leading edge hits the downstream edge to break into several small vortices, some of which flow into the cavity while some flow along the wall. The vortex at the leading edge is absorbed into the main vortex at the rear of the cavity. Therefore, the interaction between the shear layer and the main vortex governs the flow characteristics based on the feedback mechanism.

Fig. 5 shows a pressure distribution of one cycle in the x-direction at the height of $y=1.022D$. The time is the same as that depicted in Fig. 4. The locations of the leading edge and the downstream edge are at $x=9$ and 11.5, respectively. In all cases, abrupt changes can be seen to have occurred around the downstream edge of $x=11.5$. The pressure change at the downstream edge shows the impact of the vortex flowing out of the shear layer.

On the other hand, Fig. 6 shows the pressure change at the downstream edge of the two- and three-dimensional cavities for the case of the aspect ratio (L/D) = 2.5 and $M= 0.53$. After t=100, the flow converges to a cyclic steady state. The graph shows that the cyclic period is about $T_P=5.78$ for the three-dimensional case, and the time for the two-dimensional case is larger than that for the three-dimensional case. The pressure change cycle in Fig. 6 displays the dominant frequency characteristics.

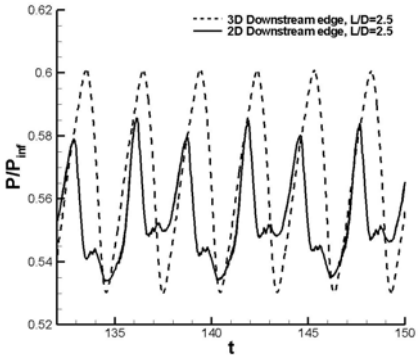

Fig. 6. Two- and three-dimensional pressure history at the downstream edge.

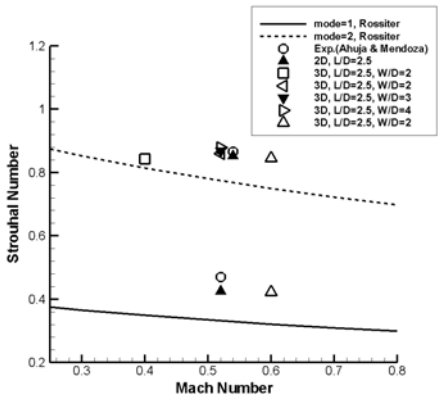

Fig. 7. Non-dimensional resonant frequencies as a function of the Mach number.

These characteristics can be understood more deeply in Figs. 8 and 9, which analyze the dominant frequencies of mode 1 and mode 2 mentioned in Ahuja and Mendoza's [8] experiment and in Rossiter's [3] equation.

In Fig. 7, the Strouhal numbers of the present work are compared with the results of Ahuja and Mendoza's [8] experiment and those of Rossiter's [3] equation. The equation has an advantage of predicting the frequency only if the Mach number and the aspect ratios of the cavities are given. However, it has a relatively large error potential, approximately 20%, in many cases [13]. The lines show the St numbers of the Rossiter equation according to the Mach number when mode(n)=1 and mode(n)=2; (○) shows the test results in Ahuja and Mendoza [8] for the cavity with an aspect ratio (L/D) of 2.5. The numerical results for the two-dimensional cavity of $L/D=2.5$ almost agree with the results of modes 1 and 2 in Ahuja and Mendoza [8].

However, in the case of the three-dimensional flow of *L/D = 2.5*, the result of mode 2 agrees with Ahuja and Mendoza [8], but there is no frequency for mode 1. There are St numbers of modes 1 and 2 at a high Mach number, but there is no St number for mode 1 at a low Mach number. In other words, there are modes 1 and 2 in the two-dimensional flow, but it depends on the Mach numbers in the three-dimensional flow. To obtain a detailed analysis of the dominant frequencies, an SPL analysis was conducted on the various aspect ratios and span wise ratios.

For the two-dimensional case in Fig. 8, the dominant frequencies corresponding to modes 1 and 2 appear at around 500 Hz and 1,000 Hz, respectively, for all aspect ratios. Fig. 9 shows the frequency characteristics for the three-dimensional case. The dominant frequency corresponding to mode 2 appears at around 800 Hz ~ 950 Hz. As the width increases, the frequency of mode 1 appears very weak. When the aspect ratio is 4.5, the dominant frequency corresponding to mode 1 clearly appears at around 500 Hz for all cases of *W/D*. Based on this phenomenon, it can be predicted that only the dominant frequency of mode 2 appears when both of *L/D* and *W/D* are small in the three-dimensional flow. Even if L/D is small, the dominant frequency of mode 1 appears for the case of a large *W/D*.

Fig. 10 shows the SPL distribution at the center of downstream edge for the aspect ratios (*L/D*) of 5.5, 6.5, and 7.5 and *W/D* of 2.0. Compared with the case of *L/D = 4.5* and *W/D = 2.0* in Fig. 9, there is one more dominant frequency below the dominant frequency of approximately 500 Hz. When the *L/D* becomes larger, the intensity of the dominant low frequency becomes stronger, similar to the intensity of the main dominant frequency. This shows that there would be another dominant low frequency due to some other reasons except for the dominant frequency of the feedback mechanism.

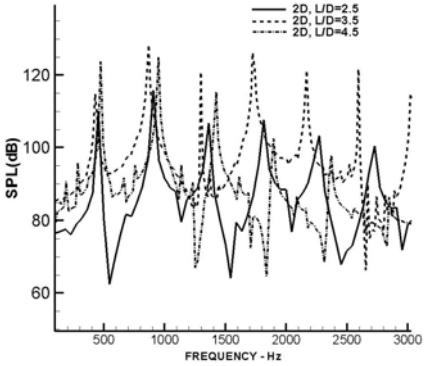

Fig. 8. SPL distribution for two-dimensional flows with aspect ratios (*L/D*) of 2.5, 3.5, and 4.

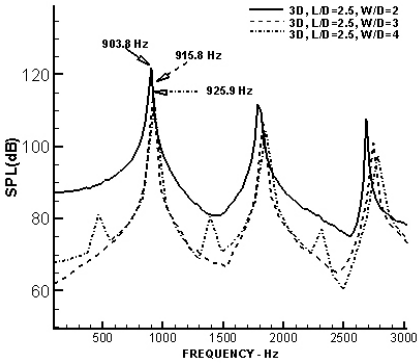

Fig. 9(a). SPL distribution for three-dimensional flows with an aspect ratio (*L/D*) of 2.5.

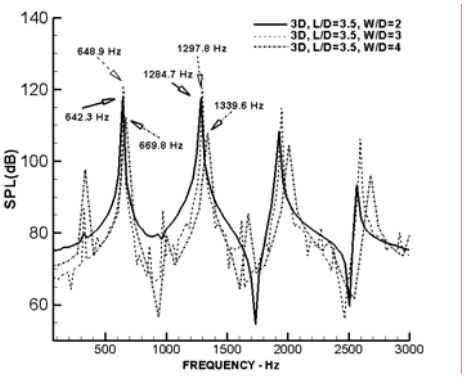

Fig. 9(b). SPL distribution for three-dimensional flows with an aspect ratio (*L/D*) of 3.5.

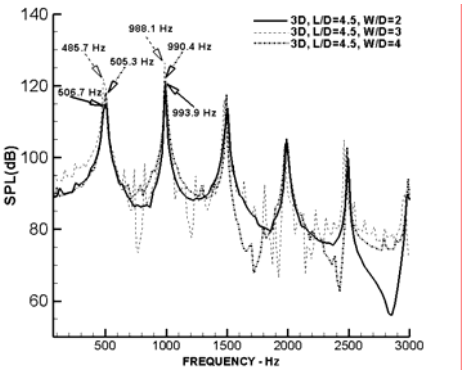

Fig. 9(c). SPL distribution for three-dimensional flows with an aspect ratio (*L/D*) of 4.5.

Fig. 11 shows the streamlines formed during a period of the cycle at the center section for the case of *L/D = 6.5* and *W/D = 2.0*. When the *L/D* is 2.5 (refer

to Fig. 5), the dominant frequencies of the shear layer are generated by the large vortex flowing into the cavity from the trailing edge. When the *L/D* increases to 6.5, the large vortex at the downstream and the small vortex in the middle section are the same as those with the *L/D* of 2.5, and another large vortex is generated at the upstream of the cavity. This clearly shows that the shear layer at the leading edge flows downstream for a while without any severe fluctuation. This also shows that there is an area wherein the large vortex from the trailing edge does not affect due to the long distance from the trailing edge. Furthermore, the shear layer starts vibrating in the middle of the area, which is a characteristic of a large *L/D* cavity. Thus, based on the frequency analysis in Fig. 11, there would be a dominant frequency of 500 Hz generated by the vortex hitting at the trailing edge and another dominant low frequency generated on the shear layer of the middle area.

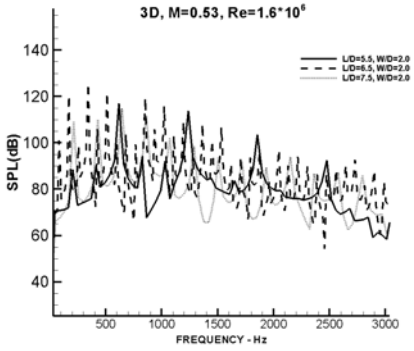

Fig. 10. SPL distribution for three-dimensional flows with aspect ratios (*L/D*) of 5.5, 6.5, and 7.5.

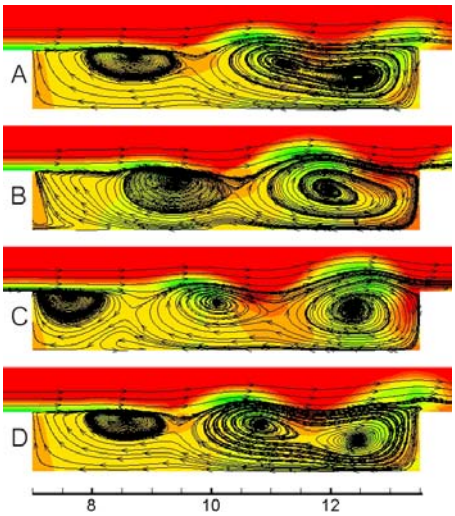

Fig. 11. Streamlines and density contours at the center section of the three-dimensional cavity (*L/D*=6.5).

The characteristics of the dominant frequency, depending on the Mach number, *L/D,* and *W/D,* can be summarized as follows. Basically, the dominant frequencies of mode 1 and mode 2 appear in the two-dimensional flow. In the three-dimensional flow, at a low Mach number and *L/D*, the frequency of mode 1 does not appear when the *W/D* is small, but the mode 1 and 2 frequencies appear. This is very similar to the two-dimensional case wherein the *W/D* becomes larger. The reason why the mode 1 frequency does not appear when the *W/D* is small is due to the vibration suppression occurring by the side wall. When the Mach number is large, the mode 1 and 2 frequencies appear regardless of the size of the *W/D*. When the *L/D* is very large, the mode 1 and 2 frequencies appear due to the feedback mechanism. Finally, the dominant low frequency appears due to the vortex generated around the leading edge of the cavity.

Figs. 12 and 13 show the CPD analyzed by Eq. (2) [15]. The figures show the correlation of pressures

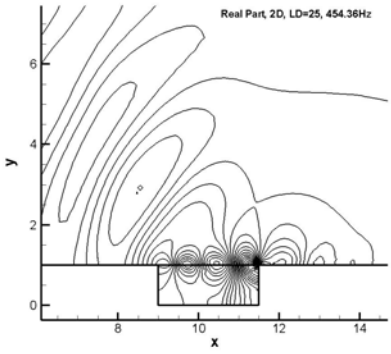

Fig. 12(a). Contours of the real part of the CPD of mode 1 for the two-dimensional cavity with an aspect ratio of 2.5.

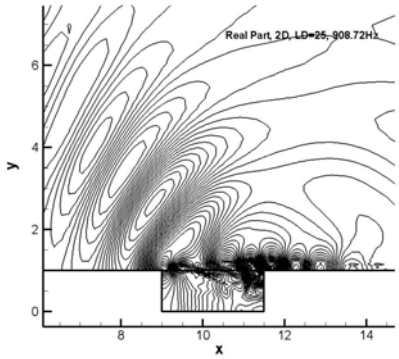

Fig. 12(b). Contours of the real part of the CPD of mode 2 for the two-dimensional cavity with an aspect ratio of 2.5.

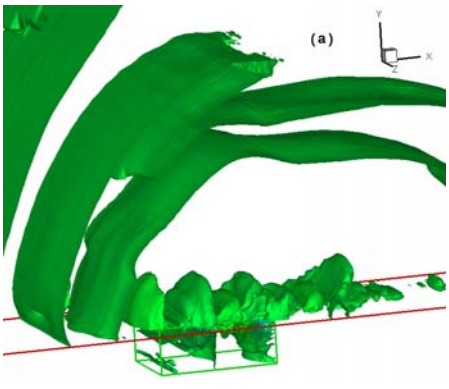

(a) mode 2 for the case of *L/D*= 2.5 and *W/D*=2

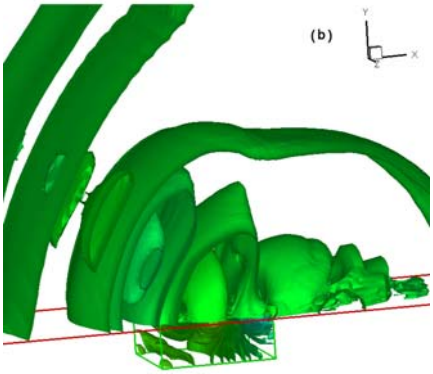

(b) mode 1 for the case of *L/D*= 4.5 and *W/D*=2

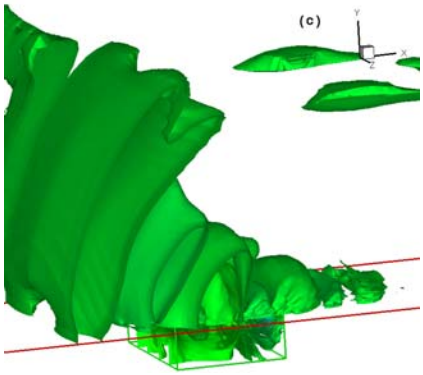

(c) mode 2 for the case of i= 4.5 and *W/D*=2

Fig. 13. Contours of the real part of the CPD for the three-dimensional cavity.

between a reference point and other regions. The analysis of CPD is similar to the Discrete Fourier Transformation (DFT) analysis carried out by Rowley, Colonius, and Basu [14]. Although the DFT results show only the magnitude of the disturbed density of the dominant frequencies in the acoustic field, the results of the CPD show the propagation and dissipation of the acoustic waves generated at or passed at the reference point. The center of the downstream edge is chosen as a reference point because the main source of the acoustic wave is the shear layer impacted to the downstream edge. The dominant frequencies of mode 1 and mode 2 are analyzed by SPL for the reference point. The correlations of the pressures between the reference point and other regions are then calculated by Eq. (2) for the frequencies of modes 1 and 2, respectively. The results of the CPD show the propagation characteristics of the frequencies for other regions. Figs. 12(a) and 12(b) show the Re(CPD) of mode 1 and mode 2 for the two-dimensional case of *L/D=2.5*, respectively. Fig. 13(a) shows only the results of mode 2 for the three-dimensional case of *L/D=2.5* and *W/D=2.0* because this case only has the dominant frequency of mode 2, as seen in Fig. 9(a). Figs. 13(b) and 13(c) show the results of modes 1 and 2 for *L/D=4.5* and *W/D=2.0*. These figures show the characteristics of the propagation of acoustic waves.

4. Conclusion

Using the unsteady compressible RANS equation with the $k-\omega$ turbulence model, the flow around a three-dimensional cavity was analyzed for the presenece of shear layer, vortex flow, acoustic waves, and so on. The Mach number of 0.4~0.6, *L/D* of 2.5 ~ 7.5, *W/D* of 2 ~ 4 and Reynolds number of 1.6×10^6 were the flow conditions. The dominant frequencies were compared with the St number of Rossiter's [3] and Ahuja and Mendoza's [8] results. It was discovered that the dominant frequencies corresponding to modes 1 and 2 for the two- and three-dimensional flows were almost the same as the frequency for a large aspect ratio. However, when the aspect ratio was small, the dominant frequency of mode 1 appeared only in the case of a large W/D of the three-dimensional flow. This was because the vibrations were suppressed by the side walls in the case of small *W/D*. For the low *L/D*, the dominant frequency was decided by the vortex flowing from the trailing edge and the feedback mechanism of the interaction between the shear layer and the vortex. For the large *L/D*, there existed dominant frequency characteristics generated due to the feedback mechanism similar to the case of low *L/D,* as well as low frequency characteristics due to another vortex generated around the

leading edge of the cavity. The results of the CPD showed the characteristics of the acoustic wave propagation of modes 1 and 2.

Reference

[1] Xin Zhang and John A. Edwards, Experimental Investigation of Supersonic Flow over Two Cavities in Tandem, *AIAA J.* 30(3) (1992).

[2] K. Krishnamurty, Acoustic radiation from two-dimensional rectangular cutouts in aerodynamic surfaces, *NACA*, (1955) TN-3487.

[3] J. E. Rossiter, Wind-tunnel experiments on the flow over rectangular cavities at subsonic and transonic speeds, *Aeronautical Research Council Reports and Memoranda* (1964) 3438.

[4] H. H. Heller, D. G. Holmes and E. E. Covert, Flow-induced pressure oscillations in shallow cavities, *Journal of Sound and Vibration*, 18 (1971) 545-553.

[5] M. Gharib and A. Roshko, The effect of flow oscillations on cavity drag, *Journal of Fluid Mechanics,* 177 (1987) 501-530.

[6] M. S. Chingwei and J. M. Philip, Comparison of Two- and Three-Dimensional Turbulent Cavity Flows, *AIAA* (2001) A01-16385.

[7] J. W. Kim and D. J. Lee, Generalized Formulation and Application of Characteristic Boundary Conditions. *4th AIAA/CEAS Areoacoustics Conference*, (1998) AIAA 98-2222.

[8] K. K. Ahuja and J. Mendoza, Effects of cavity dimensions, boundary layer, and temperature in cavity noise with emphasis on benchmark data to validate computational aeroacoustics codes, *NASA*, (1995) CR-4653.

[9] K. C. Hoffmann and S. T. Chiang, *Computational Fluid Dynamics for Engineers*, Engineering Education System USA. (1993).

[10] D. C. Wilcox, Reassessment of the Scale Determining Equation for Advanced Turbulence Models, *AIAA journal*, 19(2) (1988) 248-251.

[11] J. E. Bardina, P. G. Huang and T. J. Coakley, Turbulence Modeling Varidation, Testing, and Development, *NASA* , (1997) TM-110446.

[12] C. S. Abdol-Hamid, B. Lakshmanan and J. R. Carlson, Application of Navier-Stokes Code PAB3D With Turbulence Model to Attached and Separated Flows, *NASA*, (1975) Technical Paper-3480.

[13] T. Colonius, A. J. Basu and C. W. rowley, Numerical investigation of the flow past a cavity, *AIAA*, 99 (1999) 1912.

[14] Clarence W Rowley, Tim Colonius and Amit J. Basu, On self sustaioned oscilaation in two diemensional compressible flow over rectangular cavities, *Journal of Fluid Mech*. 455 (2002) 315-346.

[15] Woo Chel-hun, Kim Jae-soo and Lee Kyung-hwan, Three dimensional effects of supersonic cavity flow dut to the variation of cavity aspect and width ratios, *Journal of Mechanical Science and Technology* 22 (2008) 590-598.

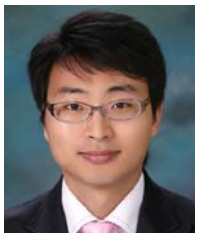

Hong-il CHOI received the B.S and M.S degrees in Aerospace Engineering from Chosun University, Korea in 2005 and 2008, respectively. He currently work at KOREA Electric Power Research Institute in Korea

Pa-ul MUN received the B.S in Aerospace Engineering from Chosun University, Korea in 2008. He is currently Candidate for the degree of master of Aerospace Engineering at Chosun University in Korea.

Jae-soo KIM received the B.S in Aerospace Engineering from Seoul National University in Korea in 1981. He then received his M.S and Ph.D. degree in Aerospace Engineering from KAIST in Korea in 1983 and 1987, respectively. He spent one year at Cornell university(USA) as a Post Doc. He worked at Korea Aerospace Research Institute for eight years. Dr. Kim is currently a Professor at the Department of Aerospace Engineering at Chosun University in Korea